

# New Phase Diagram of Relaxor Ferroelectric $(1-x)\text{Pb}(\text{Zn}_{1/3}\text{Nb}_{2/3})\text{O}_3-x\text{PbTiO}_3$

D. La-Orauttapong<sup>1</sup>, B. Noheda<sup>2</sup>, Z.-G. Ye<sup>3</sup>, P.M. Gehring<sup>4</sup>, J. Toulouse<sup>1</sup>, D.E. Cox<sup>2</sup>, and G. Shirane<sup>2</sup>

<sup>1</sup>*Department of Physics, Lehigh University, Bethlehem, PA 18015, USA*

<sup>2</sup>*Brookhaven National Laboratory, Upton, NY 11973, USA*

<sup>3</sup>*Department of Chemistry, Simon Fraser University, Burnaby, BC V5A 1S6, Canada*

<sup>4</sup>*NIST Center for Neutron Research, NIST, Gaithersburg, MD 20899, USA*

Recently, a new orthorhombic phase has been discovered in the ferroelectric system  $(1-x)\text{Pb}(\text{Zn}_{1/3}\text{Nb}_{2/3})\text{O}_3-x\text{PbTiO}_3$  (PZN- $x$ PT) for  $x=9\%$ , and for  $x=8\%$  after the application of an electric field. In the present work, we report synchrotron x-ray measurements on higher concentrations,  $10\% \leq x \leq 15\%$ . The orthorhombic phase is found for  $x=10\%$  but not for  $x \geq 11\%$ , and thus exists only in a narrow concentration range with near vertical phase boundaries on both sides. This orthorhombic symmetry ( $M_C$ -type) is in contrast to the monoclinic  $M_A$ -type symmetry recently identified at low temperatures in the  $\text{Pb}(\text{Zr}_{1-x}\text{Ti}_x)\text{O}_3$  (PZT) system over a triangle-shaped region of the phase diagram in the range  $x=0.46-0.52$ . To further characterize this relaxor-type system neutron inelastic scattering measurements have also been performed on a crystal of PZN- $x$ PT with  $x=15\%$ . The anomalous soft-phonon behaviour (“waterfall” effect) previously observed for  $x=0\%$  and  $8\%$  is clearly observed for the  $15\%$  crystal, which indicates that the presence of polar nanoregions extends to large values of  $x$ .

## I. INTRODUCTION

Recently, a number of studies have attempted to understand the origin of the very large piezoelectric coefficients measured in perovskite oxides such as  $\text{Pb}(\text{Zr}_{1-x}\text{Ti}_x)\text{O}_3$  (PZT) and  $(1-x)\text{Pb}(\text{Zn}_{1/3}\text{Nb}_{2/3})\text{O}_3-x\text{PbTiO}_3$  (PZN- $x$ PT) near the morphotropic phase boundary (MPB). The MPB is an almost vertical phase boundary that separates the rhombohedral (R) and the tetragonal (T) regions of the phase diagram of these systems (temperature vs  $x$ ). In a study of PZN-8%PT, Park and Shrout found the piezoelectric coefficient  $d_{33}$  to exceed 2500 pC/N and strain levels reaching 1.7% induced by a field applied along [001] [1]. These ultrahigh values are an order-of-magnitude greater than those previously attainable in conventional piezoelectric and electrostrictive ceramics including PZT, currently the material of choice for high performance actuators. Several experimental and theoretical studies now indicate that these very high values are related to the presence of a particular phase.

X-ray investigations by Noheda et al. [2] and Cox et al. [3] have shown that, in addition to the known rhombohedral and tetragonal phases, a sliver of a new phase exists in the phase diagram near the MPB as shown in Fig.1 for PZT [2] and PZN- $x$ PT [3], respectively. In the PZT system, the newly identified lower-symmetry phase is of monoclinic  $M_A$  type (space group  $Cm$ ) for  $0.46 \leq x \leq 0.52$  [2], while in PZN- $x$ PT an orthorhombic (O) phase (space group  $Bmm2$ ) has been irreversibly induced by a field in an 8%PT crystal [4,5] and has also been observed in a polycrystalline sample prepared from a previously-poled crystal of 9%PT [3]. This O phase is the limiting case of a monoclinic  $M_C$  type phase (space group  $Pm$ ) when the lattice parameters  $a$  and  $c$  become equal. A true  $M_C$  phase (with  $a \neq c$ ) is observed in

PZN-8%PT during the application of an electric field [4]. Very recently, Uesu et al. [6] have also observed a true  $M_C$  phase in 9%PT following an examination of several unpoled (as-grown) as well as poled crystals with nominally the same 9% concentration. Most of these were orthorhombic O but one showed a definite monoclinic  $M_C$  distortion. This raises the very interesting possibility that, for slightly higher concentrations (e.g. 10-12%PT), the ground state is actually  $M_C$ , so that the orthorhombic 9%PT phase might logically be regarded as the end-member of the  $M_C$  region. However, as

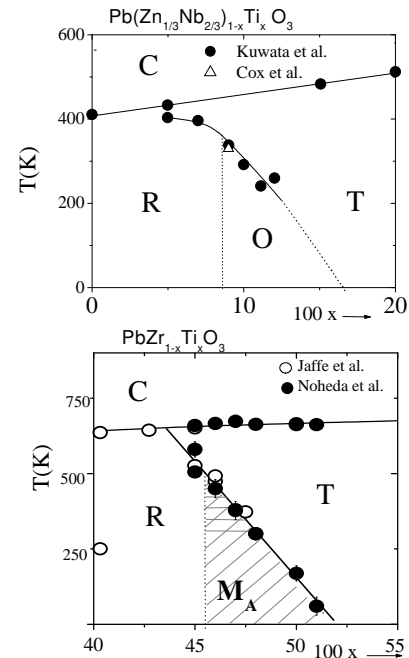


FIG. 1. Phase diagrams for PZT (bottom) and PZN- $x$ PT (top) in the vicinity of their respective MPB's, as shown in Ref. [3]

described below, the 10%PT phase has been found to be unequivocally orthorhombic ( $a = c$ ), while unexpectedly a tetragonal phase is realized at 11%PT, yielding a narrow “chimney-like” shape for the intermediate orthorhombic region.

A low-symmetry phase discovered in both PZT and PZN- $x$ PT in the vicinity of the MPB appears to be a common feature of the highly-piezoelectric perovskite systems. Recently, Vanderbilt and Cohen [7], hereafter referred to as VC, have provided a natural explanation for these recently-discovered new phases in both PZT and PZN- $x$ PT systems by extending the Devonshire theory to eighth-order. This study yields a new phase diagram for ferroelectric perovskites that includes three different types of monoclinic phases  $M_A$ ,  $M_B$ , and  $M_C$  (named after this work).

The effect of an applied electric field on the polarization has also been studied theoretically and experimentally. A polarization rotation mechanism has been proposed by Fu and Cohen [8] to explain the ultrahigh electromechanical response found in PZN- $x$ PT using  $\text{BaTiO}_3$  as a model. According to their model, the application of an electric field along the  $[001]$  direction in rhombohedral PZN- $x$ PT induces a rotation of the polarization vector in a  $(110)$  plane, from the rhombohedral to the tetragonal axis (i.e., R- $M_A$ -T). However, an experimental x-ray study by Noheda et al. on as-grown PZN- $x$ PT crystals has suggested that, as the applied electric field is increased, the polarization vector first follows this R- $M_A$ -T path but then abruptly jumps to a new path, in a plane containing the orthorhombic and tetragonal polar axes (i.e., R- $M_A$ - $M_C$ -T). [4] As the field is decreased the polarization rotates from the tetragonal  $[001]$  to the orthorhombic  $[101]$  polar directions, via the  $M_C$  phase, and the initial rhombohedral state is not recovered upon removal of the field. Recently this irreversible R- $M_A$ - $M_C$ -T polarization path has been confirmed by neutron diffraction. [9] First principle calculations by Bellaiche et al. for the rhombohedral PZT system under a  $[001]$  field also predict the R- $M_A$ - $M_C$ -T transformation, although in this case the transformation is found to be reversible. [10]

With ample experimental and theoretical evidence [11,12] for a link between the very high values of the piezoelectric and electrostrictive coefficients and the presence of a new phase, it has become essential to determine its extent in the phase diagram of PZN- $x$ PT. As mentioned above, PZN-8%PT shows the expected rhombohedral symmetry and becomes orthorhombic only after a high field has been applied, whereas PZN-9%PT clearly shows the orthorhombic symmetry ( $M_C$  with  $a = c$ ) even with no external field. [3,6] In the present paper, we have studied higher PT concentrations ( $10\% \leq x \leq 15\%$ ), using high resolution synchrotron x-ray powder diffraction. For further characterization of these relaxor systems, neutron inelastic scattering measurements have also been performed on the 15%PT crystal. The specific goal of

the inelastic measurements was to investigate the possible existence, at higher PT concentrations, of the “waterfall” shape previously observed in the soft optic mode phonon branch at lower PT concentrations. [13,14]

## II. EXPERIMENT

Single crystals of  $(1-x)\text{Pb}(\text{Zn}_{1/3}\text{Nb}_{2/3})\text{O}_3 - x\text{PbTiO}_3$  solid solution system with  $x = 10, 11, 12$  and  $15\%$  were grown by a top seeded solution growth (TSSG) technique using a PbO flux with an optimum flux ratio of 50 wt%. [15] Platelets of about 1 mm thick and 7 to 15 mm<sup>2</sup> in area were cut parallel to the reference  $(001)_{\text{cub}}$  plane and polished with fine diamond paste (down to 1  $\mu\text{m}$ ). The  $(001)_{\text{cub}}$  faces were covered with sputtered gold layers and Au-wires were attached by means of Ag-paste. The poling was performed under a field of 20 kV/cm that was applied along  $[001]_{\text{cub}}$  at 210°C (above  $T_C$ ) and maintained while cooling down to room temperature. The samples were then short-circuited for 30 min. before the electrodes were removed. For neutron inelastic scattering studies, a bigger PZN-15%PT crystal of 2.17 g in weight and 0.27 cc in volume was cut from an as-grown crystal boule with natural  $(100)_{\text{cub}}$  faces as a reference orientation.

Two types of high-resolution synchrotron x-ray powder diffraction measurements were carried out on beam line X7A at the Brookhaven National Synchrotron Light Source (NSLS) with x-rays from a Si(111) double-crystal monochromator. For the first set of measurements, an incident beam of wavelength  $\sim 0.7 \text{ \AA}$  was used and a linear position-sensitive detector was placed in the diffracted beam path. This configuration gives greatly enhanced counting rates and allows accurate data to be collected from very narrow-diameter capillary samples. The use of capillary samples helped eliminate systematic errors due to preferred orientation or texture effects. With this configuration the resulting instrumental resolution was  $\sim 0.03^\circ$  on the  $2\theta$  scale. For the second set, incident beams of wavelengths  $\sim 0.69 \text{ \AA}$  and  $\sim 0.98 \text{ \AA}$  were used with a flat Ge (220) crystal-analyzer and scintillation detector. With this type of diffraction geometry, it is not always possible to eliminate preferred orientation and texture effects, but the peak positions, on which the present results are based, are not affected. The resulting instrumental resolution is better than  $0.01^\circ$  on a  $2\theta$  scale, an order of magnitude better than that of a laboratory instrument.

The powder samples were prepared by chopping out a small fragment from the poled crystals, crushing them and loading them in a 0.2mm diameter glass capillary, as explained in Ref. [3] A closed-cycle cryostat was used for the temperature dependence measurements. The data sets were collected from 15-500 K and the sample was

rocked  $\sim 2 - 3$  degrees during the data collection, in order to achieve powder averaging.

A subsequent neutron inelastic scattering study was performed on the PZN-15%PT single crystal using both the BT2 and BT9 triple-axis spectrometers at the NIST Center for Neutron Research (NCNR). The (002) reflections of highly-oriented pyrolytic graphite (HOPG) crystals were used for both monochromator and analyzer. An HOPG transmission filter was used to eliminate

the momentum transfer  $\vec{Q} = \vec{k}_i - \vec{k}_f$  ( $k = 2\pi/\lambda$ ) fixed and varying the energy transfer  $\Delta E$ .

### III. ORTHORHOMBIC PHASE IN PZN- $x$ PT

Based on the diffraction data reported in the previous study [3] on a polycrystalline sample of PZN- $x$ PT with  $x=9\%$ , a modification of the PZN- $x$ PT phase diagram

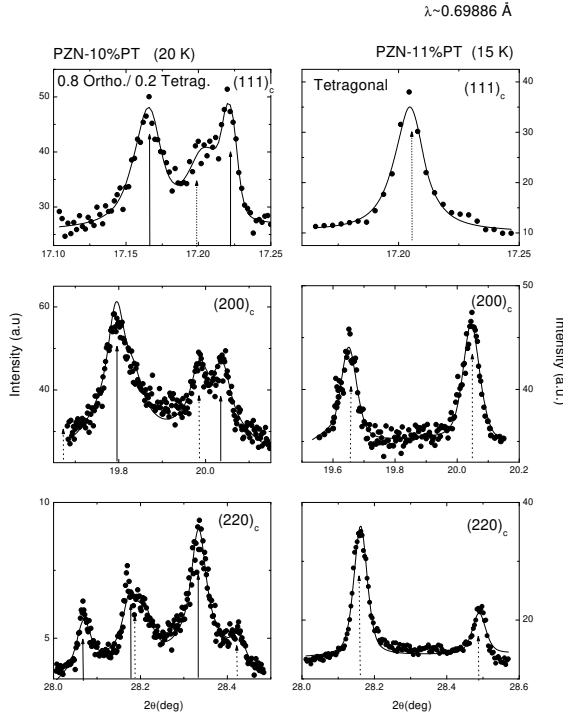


FIG. 2. Diffraction patterns of pseudo-cubic (111), (200) and (220) for PZN-  $x$ PT for  $x = 10\%$  (left) at 20 K and  $x = 11\%$  (right) at 15 K, showing the diffraction spectra for the orthorhombic and tetragonal phases.

higher-order neutron wavelengths. These measurements were made in the phonon creation mode with a fixed final energy of 14.7 meV ( $\lambda_f=2.36\text{\AA}$ ) while varying the incident neutron energy  $E_i$ . The horizontal beam collimation used was  $40' - 40' - S - 40'$ -open and  $40' - 20' - S - 20' - 80'$ . The crystal was mounted on a boron nitrate cylinder held in a goniometer, and oriented with its [001] axis vertical, thereby giving access to the (HK0) scattering zone. It was then loaded into a vacuum furnace capable of reaching temperatures up to 670K. Data were collected in the temperature range 200-650K using two types of scans. First, constant energy scans were performed by keeping the energy transfer  $\hbar\omega=E_i - E_f$  fixed while varying the momentum transfer  $\vec{Q}$ . Second, constant- $\vec{Q}$  scans were performed by hold-

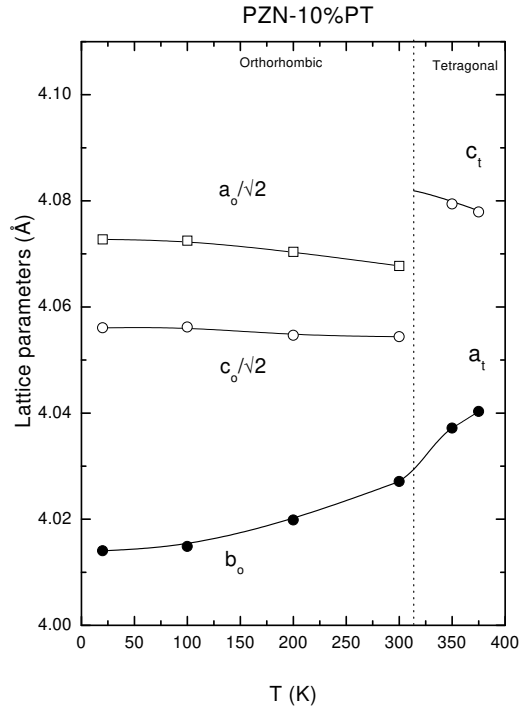


FIG. 3. Temperature dependence of the lattice parameters for PZN- $x$ PT ( $x= 10\%$ ) from 15 K to 375 K, for the orthorhombic ( $a_o$ ,  $b_o$  and  $c_o$ ) and tetragonal ( $a_t$  and  $c_t$ ) phases.

has been proposed which includes the new orthorhombic phase (O) around its MPB shown in Fig.1. However, the proposed stability region for the new O phase is limited so far to only one composition. In the present work, we have determined the full extent of the O phase by studying higher concentrations,  $x=10, 11, 12$ , and 15%. The results obtained give a comprehensive picture of the new orthorhombic phase in the PZN- $x$ PT phase diagram.

Selected regions of the diffraction profiles around the pseudo-cubic(111), (200) and (220) reflections, are plotted in Fig.2 for  $x = 10\%$  (left) and  $x = 11\%$  (right) at 20 and 15 K, respectively, showing very distinctive features for these two adjacent compositions. From the splitting and relative intensities of these profiles the symmetry of the samples can be reliably established. The  $x= 10\%$  peak profiles are very well-resolved and show

the clear pattern of an orthorhombic distortion with a residual tetragonal phase. The pseudocubic  $(111)_c$  reflection consists of two peaks corresponding to the  $(012)$  and  $(210)$  orthorhombic reflections and a third central peak corresponding to the residual tetragonal  $(111)$  singlet. Three peaks are observed around the pseudocubic  $(200)_c$  reflection corresponding to the orthorhombic  $(202)$ - $(020)$  doublet and the tetragonal  $(200)$  reflection. The pseudocubic  $(220)_c$  reflection consists of a triplet, the orthorhombic  $(004)$ - $(400)$ - $(222)$ , plus the  $(202)$ - $(220)$  tetragonal doublet. From the intensity ratios one can estimate the fraction of tetragonal phase to be about 20% of the sample volume. For the  $x=11\%$  composition, the peak profiles are clearly those of a pure tetragonal phase with a single  $(111)$  reflection and two doublets,  $(002)$ - $(200)$  and  $(202)$ - $(220)$ . The fits of these profiles show that for  $x=10\%$  the orthorhombic unit cell has  $a_o = 5.760 \text{ \AA}$ ,  $b_o = 4.014 \text{ \AA}$ ,  $c_o = 5.736 \text{ \AA}$  and the second tetragonal phase has  $a_t = 4.024 \text{ \AA}$ ,  $c_t = 4.091 \text{ \AA}$ . For  $x=11\%$  the tetragonal unit cell parameters are  $a_t = 4.018 \text{ \AA}$ ,  $c_t = 4.113 \text{ \AA}$ .

peratures, the orthorhombic lattice parameter  $b_o$  steadily increases while the  $c_o/a_o$  ratio decreases only slightly. At temperatures between 325 and 375 K, the symmetry is found to be tetragonal with lattice parameters  $a_t$  and  $c_t$ . The sudden change in the  $a_o$  and  $c_o$  lattice parameters at around 325 K establishes the first-order character of the orthorhombic-tetragonal phase transition. The residual tetragonal phase found for  $x=10\%$  could have an intrinsic character since a certain degree of phase coexistence is expected in a first-order phase transition. The overall behaviour is identical to that previously reported for  $x=9\%$  [3]. Similar temperature-dependence studies have been conducted for higher concentrations and the results are shown in Fig. 4. The lattice parameters as a function of temperature reveal a cubic-tetragonal phase transition for  $x=15\%$  (top) and for  $x=12\%$  (bottom). At low temperature, the system is purely tetragonal. With increasing temperature, the strain ratio  $c_t/a_t$  decreases, while approaching the transition to the cubic phase at  $\approx 490 \text{ K}$  and  $\approx 475 \text{ K}$ , for  $x=15$  and  $12\%$  respectively. As shown in Figs.3,4 and also in Ref. [3], the cubic phase

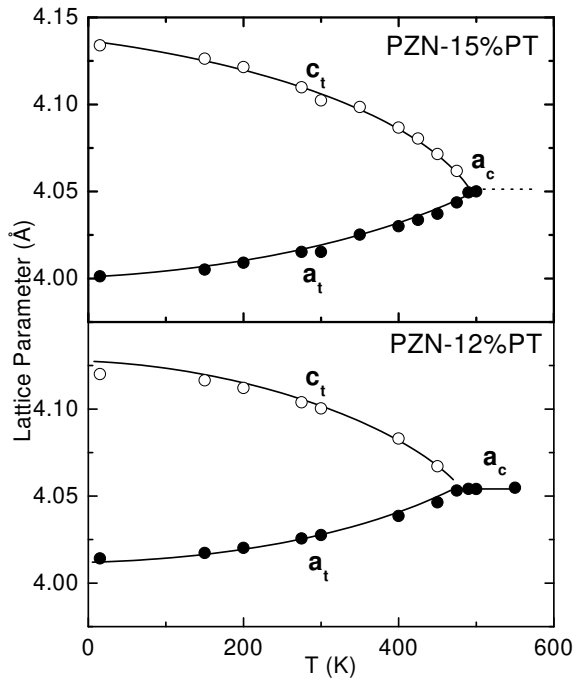


FIG. 4. Lattice parameters vs. temperature for PZN- $x$ PT for  $x=15\%$  (top) and  $12\%$  (bottom) over the whole temperature range from 15 K to 550 K, showing the tetragonal ( $a_t$  and  $c_t$ ) to cubic ( $a_c$ ) phase transition.

The evolution of the lattice parameters with temperature for  $x=10\%$  reveals an orthorhombic-to-tetragonal phase transition, as shown in Fig.3. At increasing tem-

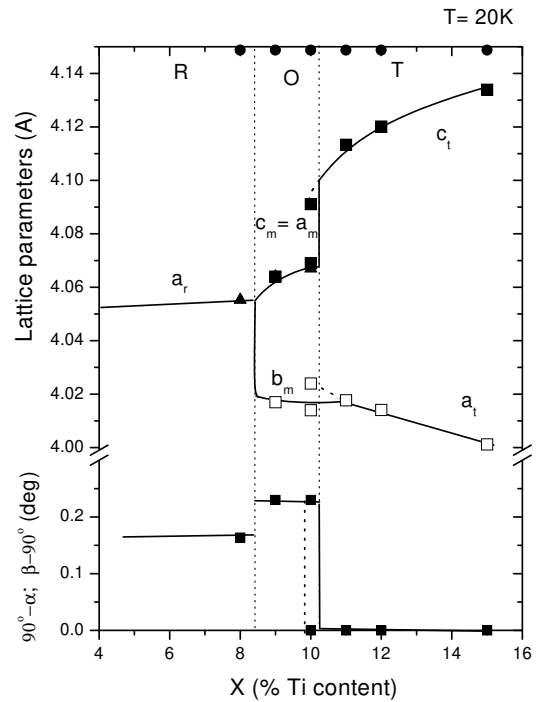


FIG. 5. Lattice parameters vs. Ti concentration at 20 K for the rhombohedral ( $a_r$  and  $\alpha$ ), monoclinic ( $a_m, b_m, c_m$  and  $\beta$ ) and tetragonal ( $a_t$  and  $c_t$ ) phases from the results of this work, including data from Refs. [3,4].

was reached for the tetragonal samples at the expected temperatures; however a single cubic phase is not observed below 500K for the orthorhombic  $x=9-10\%$  sam-

ples. The reason for this is a purely technical one: in the latter samples, the large grain size of the powders ( $\sim 40\mu\text{m}$ ) prevented good thermal contact between the grains inside the capillary, and a uniform high temperatures could not be reached. In the case of the tetragonal samples the grain size was much smaller and good thermal contact was attained.

The lattice parameters as a function of composition at 20 K are presented in Fig.5, which includes the concentrations studied in this work, as well as the previous data reported in Refs. [3,4] for  $x=8\%$  and  $9\%$ . This figure shows the structural evolution from the rhombohedral to the tetragonal phase via the orthorhombic phase. For  $x \leq 8\%$  the crystals exhibit the expected rhombohedral symmetry. For  $x \geq 11\%$ , the expected tetragonal symmetry is found with the strain ratio  $c_t/a_t$  increasing from 1.0237 at  $x=11\%$  to 1.0331 at  $x=15\%$ . However, between  $9\% \leq x \leq 10\%$ , the symmetry is found to be orthorhombic.

#### IV. SOFT PHONON ANOMALIES IN PZN- $x$ PT

A series of neutron inelastic measurements were subsequently performed on the PZN-15%PT single crystal to study the so-called “waterfall” feature, first observed in PZN-8%PT [13], and later in PZN [14], at higher concentrations of  $\text{PbTiO}_3$ . Specifically, we wished to determine whether or not this waterfall feature persisted beyond the MPB. The waterfall is an anomaly of the lowest-frequency transverse optic (TO) phonon branch that is correlated with the condensation, at  $T = T_d$ , of local regions of randomly-oriented polarization, also known as polar nanoregions (PNR), which disrupt the propagation of long-wavelength TO polar modes. The existence of  $T_d$ , which can be hundreds of degrees higher than  $T_c$ , was first reported by Burns and Dacol for a variety of systems including both PZN and PMN. [16] Because the PNR are polar, they naturally couple to the polar TO phonon mode, which in turn can serve as a microscopic probe of the PNR. Their presence is manifested by a drastic broadening of the TO phonon energy linewidth below a specific wavevector, and gives rise to a steep ridge of scattering when plotted as a function of wavevector  $q$  as the long-wavelength phonon cross section becomes distributed in energy. The search for the waterfall feature should thus yield important information about the possible existence of the PNR beyond the MPB.

Examples of two constant- $E$  scans for  $\hbar\omega = 7\text{ meV}$  measured along the [010] cubic direction taken in the low temperature phase (400 K) and in the higher temperature phase (650 K) are shown in Fig. 6. The solid lines are Gaussian fits that show the peak position or a ridge of scattering intensity shifted to smaller  $q$  as the

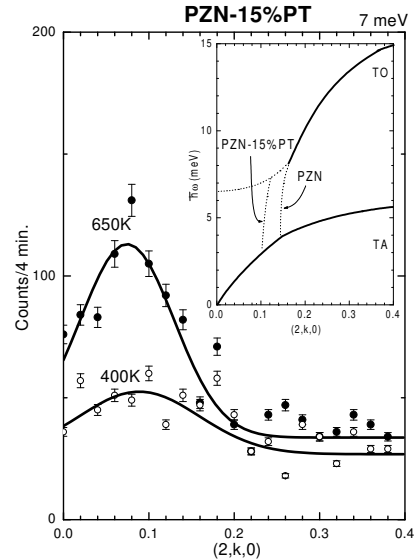


FIG. 6. Constant- $E$  scans at 7 meV (phonon creation) measured at 400 K and 650 K on a PZN-15%PT crystal. Inset shows the dispersion curves for the TA and the lowest-energy TO modes, showing the anomalous behavior of PZN- $x$ PT. The data from Ref. [14] are also included and shown by two vertical dot lines.

temperature increases. These data, shown schematically in the inset of Fig.6, suggest that the ridge of scattering evolves into the expected TO phonon branch behavior at higher temperature. In the inset of Fig.6, the solid lines represent dispersions of the transverse acoustic (TA) and the lowest-frequency TO phonon branches whereas the dashed lines show the presence of the steep ridge of scattering intensity at  $q \sim 0.1$  reciprocal lattice units (r.l.u.) for PZN-15%PT and 0.14 r.l.u. for PZN at a temperature of about 500 K (see Ref. [14]). It is interesting to note that the appearance of the steep ridge of scattering is shifted towards the zone-center i.e.,  $(2,0.14,0)$ ,  $(2,0.13,0)$  and  $(2,0.1,0)$  for  $x=0, 8$  and  $15\%$ , respectively with increasing PT concentrations. So far 15%PT is the highest concentration that we have studied, and it is possible that the higher concentrations might show a softening of a zone-center TO phonon as observed in the conventional ferroelectric PT [17], which would established the end member of the waterfall. This indicates that the anomalous soft phonon behavior is not simply a feature of compositions near the MPB but is extended to large values of  $x$ . It must be related to the presence of polar nanoregions rather than to the newly discovered phases. Therefore, the microstructural characters of relaxor fer-

roelectrics are retained to some degrees in the PZN- $x$ PT solid solution systems up to a quite high concentration of PT beyond the MPB.

## V. DISCUSSION

It now becomes clear that the presence of the new phase at the MPB in the PZN- $x$ PT phase diagram has orthorhombic rather than monoclinic symmetry. However, the orthorhombic cell observed here can be regarded as a doubled monoclinic cell of the  $M_C$  type (space group Pm) in the limit of  $a = c$ , as discussed in Ref. [4]. This is not the same type of monoclinic distortion  $M_A$  that was observed in the PZT system, which has Cm symmetry. [2] The  $M_A$  type has  $b_m$  directed along the pseudo-cubic [110] direction, while in  $M_C$   $b_m$  is directed along the pseudo-cubic [010].

In order to understand how the symmetry of the newly discovered phases facilitates the polarization rotation, it is useful to compare PZN- $x$ PT with BaTiO<sub>3</sub>. However, there is the question whether the new PZN- $x$ PT orthorhombic cell is fundamentally different from the old BaTiO<sub>3</sub> orthorhombic cell, both with the same space

energy barrier existing in PZN- $x$ PT, between the O and the  $M_C$  states, which allows the O polar axis [101] to rotate easily in the monoclinic plane.

The high-resolution synchrotron x-ray powder diffraction study of PZN- $x$ PT ( $10\% \leq x \leq 15\%$ ) as a function of temperature has allowed us to define the new orthorhombic region of the phase diagram. We show that the low-temperature orthorhombic structure of PZN- $x$ PT is found for  $x = 10\%$  but not for higher concentrations. With the results of this and earlier studies of PZN- $x$ PT ( $8\% \leq x \leq 15\%$ ), we have completed a revision of the PZN- $x$ PT phase diagram around its MPB as shown in Fig. 7. The new orthorhombic phase exists in only a narrow concentration range ( $8\% < x < 11\%$ ) between the rhombohedral and tetragonal phases with near vertical phase boundaries on both sides.

To be sure that the proposed phase diagram corresponds to the ground state of these materials, the poled/unpoled problem deserves further attention. Due to the intrinsic disorder existing in these relaxor ferroelectrics, the diffraction peaks of the as-grown samples are very broad, and to solve the true underlying structure by powder diffraction is an extremely difficult task. In order to induce the ferroelectric ordered state the samples are poled by an electric field. The extremely sharp peaks of the ordered material allow us to unequivocally determine the structure. However, due to the small energy differences between the different phases around the MPB, sometimes the poled and unpoled states of the samples do not have the same symmetry or, alternatively the symmetry can depend on the direction of the applied electric field, as in the case of the  $x = 8\%$  composition [4]. The as-grown sample is known to be rhombohedral, but an irreversible phase transition can be induced by an electric-field applied along the [001] direction, and the sample poled in such a way becomes orthorhombic. However, the initial rhombohedral state can be recovered by grinding the crystals below  $\sim 30\mu\text{m}$  [4].

In a similar way, the  $x = 9\%$  composition showed very sharp and well-defined diffraction peaks after poling, displaying a clear orthorhombic symmetry [3]. In this case, however the poled and unpoled samples do not have intrinsically different characteristics, as shown in Ref. [6], and the main difference is the existence of a residual tetragonal phase in the unpoled samples. Here it is worth mentioning that it is very difficult to grow a perfectly homogeneous crystal and that certain compositional variations are always present for the same nominal composition. In this work we have shown that the poled  $x = 10\%$  crystal behaves much like the poled  $x = 9\%$  [3], and that the poled  $x = 11-15\%$  samples are tetragonal, as expected for the as-grown samples [18]. Therefore, we believe that the new PZN- $x$ PT phase diagram contains an orthorhombic intermediate phase for  $8\% < x < 11\%$  as shown in Fig. 7, where the  $x$  values stand for the nominal compositions.

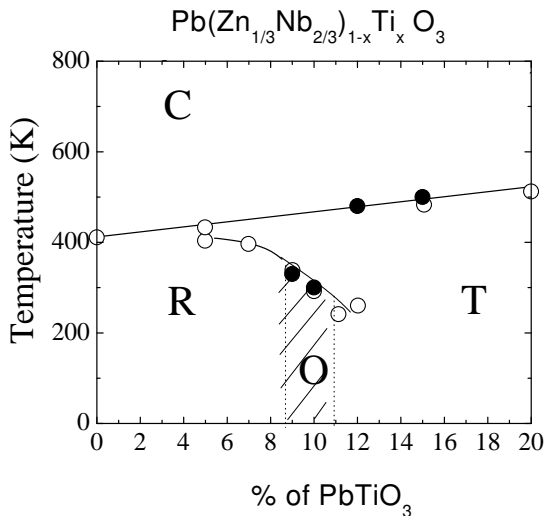


FIG. 7. Updated phase diagram of PZN- $x$ PT around its MPB. The open circles and solid lines represent the phase diagram by Kuwata et al. [18]. The results of this work, as well as those in Ref. [3] ( $x = 9\%$ ) are plotted as solid circles. The new orthorhombic phase (O) is represented by the shaded-area.

group. The difference here seems to be in the very low

For further characterization of PZN- $x$ PT, we have subsequently performed a neutron inelastic scattering on the PZN-15%PT single crystal to study the “waterfall” feature. As was the case for PZN-8%PT [13] and later for PZN [14] measured at the same temperature, an anomalous scattering ridge in PZN-15%PT is also found, but shifted closer to the zone center. It will be interesting to study the crystals of higher values of  $x$ , and then to trace the evolution of the TO modes as a function of  $x$ . Thus, the conclusion of the present study is that the waterfall phenomenon is not associated with the new low temperature phase near the MPB, but is a more general feature of the PZN- $x$ PT solid solution system, which retains some degrees of the relaxor ferroelectric characters, to be associated with the presence of the polar nanoregions.

During the preparation of this manuscript two different papers by Lu et al. [19] and Xu et al [20] have reported the optical observation of orthorhombic and monoclinic domains, respectively, in the related ferroelectric  $\text{Pb}(\text{Mg}_{1/3}\text{Nb}_{2/3})\text{O}_{3-x}\text{PbTiO}_3$  system (PMN- $x$ PT) around its MPB ( $x \simeq 0.33 - 0.35\%$ ). A third paper by Ye et al. [21] reports the existence of a monoclinic phase of  $M_A$  type in PMN-35%PT, after the application of an electric field. Work is in progress to clarify which type of low symmetry distortion occurs in the phase diagram of PMN- $x$ PT.

#### ACKNOWLEDGMENTS

We wish to thank W. Chen for an excellent job in crystal growth. Research was carried out (in part) at the National Synchrotron Light Source, Brookhaven National Laboratory, which is supported by the US Department of Energy, Division of Material Science and Division of Chemical Science. We acknowledge the support of the NIST Center for Neutron Research, U.S. Dept. of Commerce, in providing the neutron facilities used in this work. Financial support by DOE under contracts No. DE-FG02-00ER45842 and No. DE-AC02-98CH10886 and the ONR Grant # N00014-99-1-0738 is also acknowledged.

- [5] D. Viehland, J. Appl. Phys. **88**, 4794 (2000)
- [6] Y. Uesu, M. Matsuda, Y. Yamada, K. Fujishiro, D.E. Cox, B. Noheda and G. Shirane, J. Phys. Soc. Japan (submitted). Cond-mat/00106552.
- [7] D. Vanderbilt and M.H. Cohen, Phys. Rev. B. **63**, 94108 (2001).
- [8] H. Fu and R.E. Cohen, Nature **403**, 281 (2000).
- [9] K. Ohwada, K. Hirota, P.W. Rehrig, P.M. Gehring, B. Noheda, Y. Fujii, S-E. Park, and G. Shirane, J. Phys. Soc. Japan (in press). Cond-mat/0105086.
- [10] L. Bellaiche, A. García, and D. Vanderbilt, Phys. Rev. B **64**, 060103(R) (2001)
- [11] R. Guo, L.E. Cross, S-E. Park, B. Noheda, D.E. Cox, and G. Shirane, Phys. Rev. Lett. **84**, 5423 (2000).
- [12] L. Bellaiche, A. García, and D. Vanderbilt, Phys. Rev. Lett. **84**, 5427 (2000).
- [13] P.M. Gehring, S.-E. Park, and G. Shirane, Phys. Rev. Lett. **84**, 5216 (2000).
- [14] P.M. Gehring, S.-E. Park, and G. Shirane, Phys. Rev. B. **63**, 224109 (2001).
- [15] W. Chen and Z.-G. Ye, J. Crystal Growth (in press).
- [16] G. Burns and F.H. Dacol, Phys. Rev. B. **28**, 853 (1983).
- [17] G. Shirane, J.D. Axe, J. Harada, and J.P. Remeika, Phys. Rev. Lett. **2**, 155 (1970).
- [18] J. Kuwata, K. Uchino, and S. Nomura, Ferroelectrics **37**, 579 (1981).
- [19] Y. Lu, D-Y. Jeong, Z-Y. Cheng, and Q.M. Zhang, H-S. Luo, Z-W. Yin, and D. Viehland, Appl. Phys. Lett. **78**, 3109 (2001)
- [20] G. Xu, H. Luo, H. Xu, and Z. Yin, Phys. Rev. B. **64**, 020102(R) (2001).
- [21] Z.-G. Ye, B. Noheda, M. Dong, D. Cox, and G. Shirane, Phys. Rev. B. (submitted).

- 
- [1] S.-E. Park and T.R. Shrout, J. Appl. Phys. **82**, 1804 (1997).
  - [2] B. Noheda, D.E. Cox, G. Shirane R. Guo, B. Jones, and L.E. Cross, Phys. Rev. B. **63**, 14103 (2001).
  - [3] D.E. Cox, B. Noheda, G. Shirane, Y. Uesu, K. Fujishiro, and Y. Yamada, Appl. Phys. Lett **79**, 400 (2001).
  - [4] B. Noheda, D.E. Cox, G. Shirane, S-E. Park, L.E. Cross, and Z. Zhong, Phys. Rev. Lett. **86**, 3891 (2001).